Progress In Electromagnetics Research M, Vol. 62, 19–28, 2017

Continuous Beam Scanning in Substrate Integrated Waveguide Leaky Wave Antenna

Rahul Agrawal[1, *], Pravesh Belwal[1], Mahakar Singh[2], and Suresh C. Gupta[1]

Abstract—A planar substrate integrated waveguide leaky wave antenna (LWA) with cross slots is proposed in the frequency range of 10 GHz–15.5 GHz. Moreover, the symmetrical version of the structure is designed and analyzed in terms of the simulated S-parameters and E-field distribution which shows the existence of the open stopband in the frequency range from 12.91 GHz–14 GHz, consequently degrading the radiation beam at broadside. Therefore, asymmetry is introduced in the unit cell design w.r.t the position of the cross slots to achieve the continuous beam scanning in the desired frequency range. The unit cell is analyzed with the help of dispersion relation and Bloch impedance for predicting the beam scanning and matching of the proposed LWA respectively. This planar LWA is fabricated by the standard printed-circuit board process. Measured results are almost consistent with the simulation ones with a continuous beam scanning from of $-40°$ to $+16°$ with gain varying from 8.5 dBi to 11 dBi.

1. INTRODUCTION

In recent years, leaky wave antennas (LWAs) have received great attention in applications such as radar, point to point and satellite communication systems for their high directivity and beam scanning capability without the requirement of complex feeding networks [1]. The suitable platform used for developing a LWA is substrate integrated waveguide (SIW) [2–4]. SIW is a very promising waveguide structure which comes in the lifetime and maintains the advantages of a rectangular waveguide, such as high Q-factor and high power handling capability in planar form [5]. Basically in SIW, dielectric is sandwiched between two parallel conducting layers which are connected via metallic posts.

LWAs are broadly classified into three classes: uniform, periodic, and quasi periodic [6]. The uniform waveguide LWA contains a long uniform slot, and it can scan only in forward direction, excluding broadside [7], whereas the 1-D periodic LWAs offers the backward to forward beamscanning with open stopband (OSB) at broadside which is big time concern for LWA [8].

The broadside radiation problem has plagued periodic LWAs for more than four decades. A severe loss in the performance, particularly in gain and efficiency, occurs when LWAs radiates in the broadside direction (direction normal to the antenna plane). This degradation has severely restricted practical applications of these types of antennas over time. If no specific precautions are taken, an OSB occurs at broadside [9]. The OSB is associated with strong variations of the leakage constant and the input impedance over the frequency, hence it affects the radiation efficiency.

To obtain a continuous beam scanning from backward to forward direction in periodic LWAs, one needs to suppress the OSB in the periodic LWA [10]. Periodic LWA implementations with composite right/left-handed (CRLH) lines have been shown to provide continuous beam scanning radiating in their fundamental space harmonic ($n = 0$) [11–15]. Radiation in higher space harmonics could also be possible for achieving continuous beam scanning [10], but radiating in higher space harmonics generally

Received 11 September 2017, Accepted 24 October 2017, Scheduled 4 November 2017
* Corresponding author: Rahul Agrawal (rahul16389@gmail.com).
[1] Department of Electronics and Communication Engineering, DIT University, Dehradun 248009, India. [2] Defense Electronic Application Laboratory, DRDO, Dehradun 248001, India.

represents limitations of the single-beam scanning range [16]. Periodic LWAs implemented with CRLH transmission lines belongs to the quasi-periodic category ($S < \lambda g/4$), and hence there are fabrication issues [17]. In [10], a planar SIW LWA structure is designed, eliminating the OSB by introducing the longitudinal slots as parallel components. The OSB is suppressed by utilizing an impedance matched LWA unit cell.

In this paper, asymmetrical planar SIW LWA with cross slots having the capability of continuous beam scanning is proposed. Moreover, the symmetrical case of the structure is studied. A prototype of the proposed LWA is fabricated and experimentally validated. The proposed LWA prototypes are easy to fabricate owing to its single layer fabrication. The remainder of this paper is organized as follows. Section 2 provides a theoretical discussion on the bloch Impedance and propagation constants which are the keystones for designing a unit cell of periodic LWAs, whereas in Section 3 both symmetrical and asymmetrical structures are studied, and asymmetrical structure is optimized with cross slots for continuous beam scanning through broadside. Section 4 presents the measurement of a fabricated prototype which is compared with the simulated results, and finally, the conclusion is drawn in Section 5.

Research is carried out to fulfill the aim of designing planar LWA that can be integrated simply with transmitter/receiver circuits and can easily be mounted on surfaces of large bodies (satellites) without deteriorating their performance.

2. DISPERSION DIAGRAM & BLOCH IMPEDANCE

The radiation and matching properties of the periodic LWAs for the unit cell are dominantly controlled by the propagation constant (γ) and Bloch impedance (Z_B), respectively. These properties are defined by transmission matrix ($ABCD$ matrix). The $ABCD$ matrix is convenient here as the overall $ABCD$ matrix of the cascade of the two-port networks can be calculated by the multiplication of the individual $ABCD$ matrices [18, 19]. In this section, the equations for propagation constant and Bloch impedance are provided based on ABCD parameters. A periodic LWA, designed as a two-port network, is shown in Fig. 1.

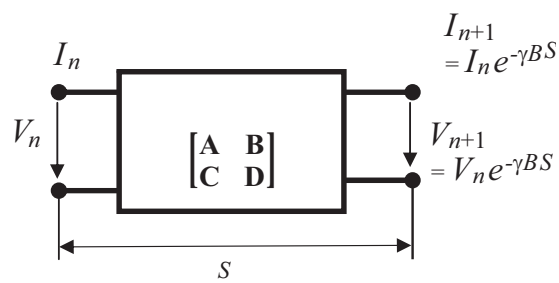

Figure 1. Equivalent two port network representation of LWA.

Since the terminal voltages and currents are the functions of the electric field, the propagation constant can be related to these quantities as

$$V_{n+1} = V_{ne^{-\gamma S}} \tag{1}$$

$$I_{n+1} = I_{ne^{-\gamma S}} \tag{2}$$

where n is an integer number referring to nth unit cell terminal. By using the $ABCD$ matrix equations, one can write

$$\begin{bmatrix} V_n \\ I_n \end{bmatrix} = \begin{bmatrix} A & B \\ C & D \end{bmatrix} \begin{bmatrix} V_{n+1} \\ I_{n+1} \end{bmatrix} = \begin{bmatrix} V_{n+1} \\ I_{n+1} \end{bmatrix} e^{\gamma S} \tag{3}$$

Assuming the LWA as a reciprocal device, the propagation constant is obtained as

$$\gamma = \frac{1}{S} \text{arccosh} \left[\frac{A+D}{2} \right] \tag{4}$$

In addition to propagation constant, another parameter, the Bloch impedance, is of paramount importance for designing the unit cell of LWA. The Bloch impedance, which predicts the matching

of the LWA is attributed to the input impedance of the infinite structure formed by a cascading of the unit cells. Basically it is the impedance at the terminals of the unit cell which is obtained in terms of $ABCD$ parameters as

$$Z_B = \frac{V_n}{I_n} = \frac{V_{n+1}}{I_{n+1}} = \frac{2B}{(D-A) + \sqrt{(A+D)^2 - 4}} \tag{5}$$

3. ANTENNA DESIGNS AND ITS ANALYSIS

The initial design of the proposed LWA starts with the design of the unit cell. The unit cell of the periodic LWA consists of two parts; SIW and the cross slots. For the resonator, the cross slot is etched on the top surface, and it is grounded by a solid metallic plane. Increasing the width and length of the slots will make the radiation more efficient. It is noted that the vias, as a short circuited stub, provide the shunt inductance. All the prototypes are built on a normally used substrate of Rogers 5880 with a permittivity of 2.2, loss tangent of 0.001 and thickness of 0.787 mm. The vias used in the models share a common diameter (D) of 1 mm and a center-to-center spacing (p) around 2 mm.

The design of a unit cell starts with the SIW. The width, diameter of vias and spacing between vias are chosen such that the proposed structure operates from 10 to 15.5 GHz [20, 21].

$$W_{SIW} = w - 1.08\frac{D^2}{p} + 0.1\frac{D^2}{w} \tag{6}$$

$$D < \lambda_g/5 \tag{7}$$

$$p < 2D \tag{8}$$

The cross slot consists of longitudinal and transverse slots for the broadside radiation to occur with radiation efficiency more than 50% [22].

3.1. Symmetrical and Asymmetrical Cases

The unit cell configurations of the asymmetrical and symmetrical cases are shown in Figs. 2(a) & (b), while the prototypes of the whole transmission line are shown in Figs. 2(c) & (d). In the latter case, the design is symmetrical w.r.t its longitudinal and transverse axis. In [23], it has been concluded that an LWA whose unit cell is symmetrical w.r.t to its longitudinal and transverse axes has a fundamental radiation efficiency limitation of 50%. Developing the array of the symmetrical unit cell, there exists a OSB around 1 GHz. Therefore, the unit cell which is asymmetrical w.r.t to its both axes is designed which overcomes the aforementioned disadvantages of symmetrical structure. The unit cell is made asymmetrical by changing the position of the slots. The size, shape, position and angle of the slots are optimized to mitigate the open stopband existing in the symmetrical case. The slots are designed according to our broadside frequency and taken as $\lambda/4$ and $\lambda/8$ for transverse and longitudinal directions, respectively. The parameters for both the cases are shown in Table 1.

Table 1. Parameters of the unit cells.

Parameters	Values (Symm)	Values (Asymm)
W_{SIW}	14 mm	14 mm
D	1 mm	1 mm
S	14.34 mm	14.34 mm
p	2.1 mm	2.1 mm
L_L	3 mm	3 mm
L_T	6 mm	6 mm
Wid	1 mm	1 mm
A_P	0 mm	2.86 mm

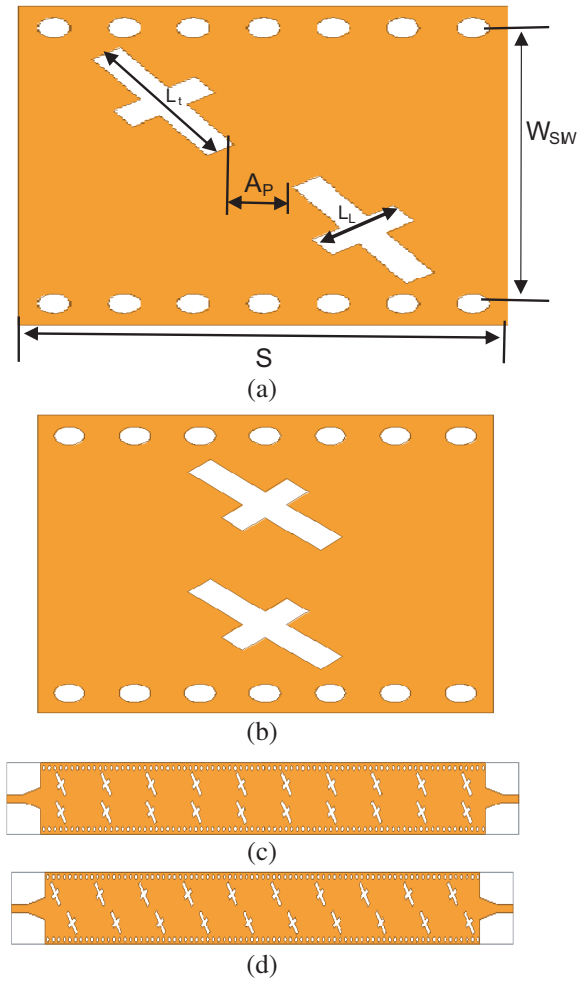

Figure 2. (a) Asymmetrical unit cell configuration, (b) symmetrical unit cell configuration, (c) overall prototype of symmetrical LWA, (d) overall prototype of asymmetrical LWA.

The phase constant, normalized to its constant in vacuum for the proposed unit cell is plotted in Fig. 3 by Ansoft's High Frequency Structure Simulator (HFSS) software package using the equation given below.

$$\beta = \frac{\text{acos}((1 - S_{11} * S_{22}) + (S_{12} * S_{21}))}{(2 * S_{21})} \tag{9}$$

The phase constant, normalized to free space wavenumber (k_o), of the unit cell is plotted using Eq. (9). The decrease and increase of phase constant indicate backward and forward directions with frequency respectively. Backward scanning range is greater than the forward scanning in the desired frequency band as seen from the dispersion curve with transition point (~ 13.5 GHz) at zero crossing point.

It is also noted that the impedance matching should also be taken into account during the design process. However, this matching can be designed in the last using a taper line at the two ends of a leaky-wave antenna. Bloch impedances for both symmetrical and asymmetrical unit cells are plotted in Fig. 4 using Eq. (10) [24]. The average real value of Bloch impedance is around 75 ohms, hence there is a mismatch confirmed in the S-parameters results of the symmetrical case, whereas it is around 50 ohms for the asymmetrical case that can be matched using a tapered line.

$$Z_B = 50 * \sqrt{\frac{(1 + S11)^2 - (S21)^2}{((1 - S11)^2 - (S21)^2}} \tag{10}$$

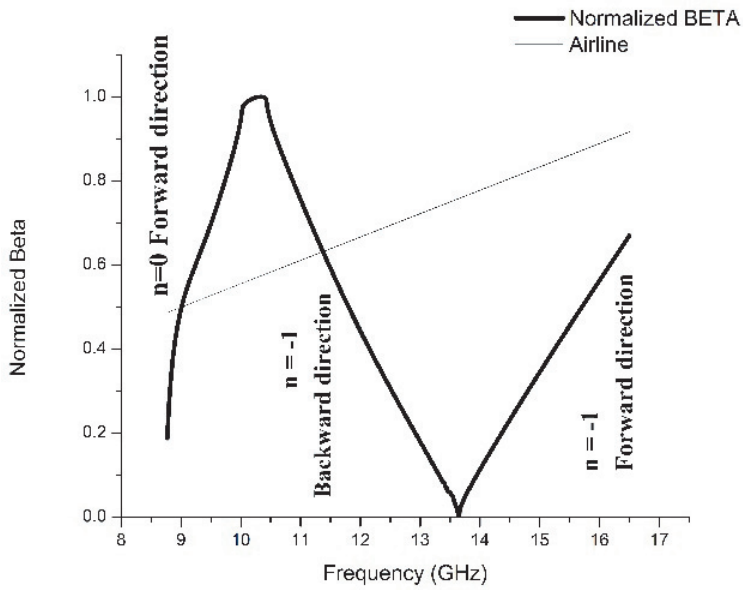

Figure 3. Simulated dispersion diagram of the unit cell of the LWA.

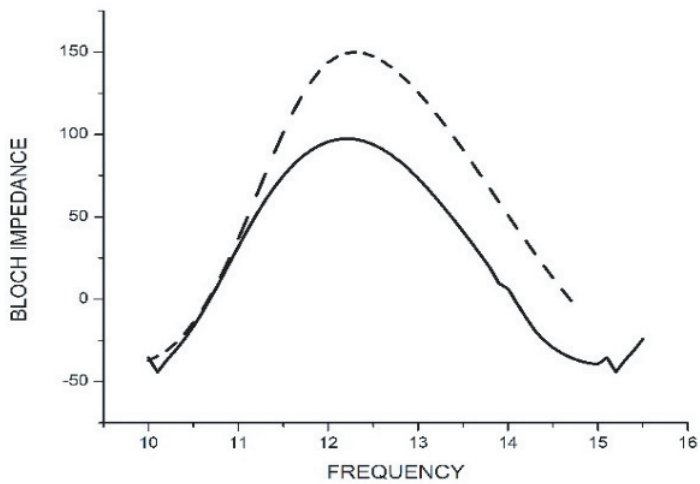

Figure 4. Bloch impedances for symmetrical (dotted) and asymmetrical (solid) unit cells.

4. RESULTS AND DISCUSSIONS

The simulated S parameters of the symmetrical case are shown in Fig. 5 which confirms the presence of the OSB from 12.91 GHz to 14 GHz.

At the frequency of broadside radiation, the reflected waves of each unit cell are in phase and are not able to cancel each other, and hence no EM power is fed into the LWA for broadside radiation. By looking into the electric field distributions plotted at different frequencies in Fig. 6, it is observed that at transition frequency (13.5 GHz), no power is fed in LWA structure which confirms the OSB behavior for the symmetrical case.

For verification purpose, fabricated asymmetrical case of the LWA designed in Section 3 is shown in Fig. 7. This prototype is fed by SMA connectors through microstrip-to-SIW transitions. The prototype is fabricated using Rogers 5880 ($\varepsilon_r = 2.2$) substrates. The S-parameters are measured using a microwave vector network analyzer (VNA), and the results are depicted in Fig. 8, together with the simulation

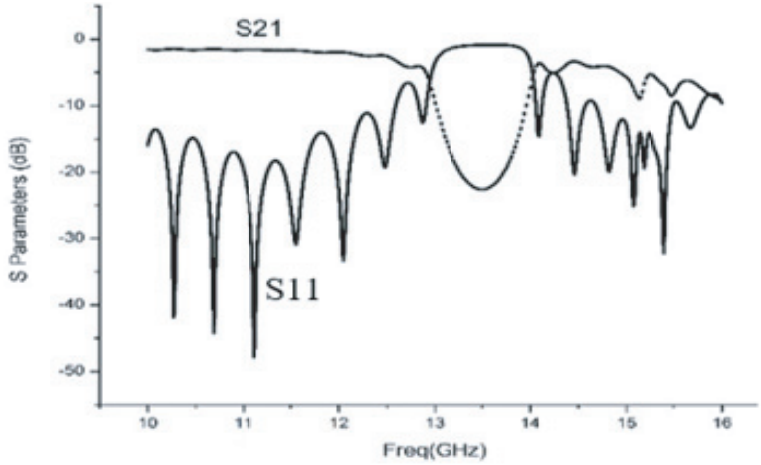

Figure 5. Simulated spectral responses of the magnitudes of S parameters for symmetrical case.

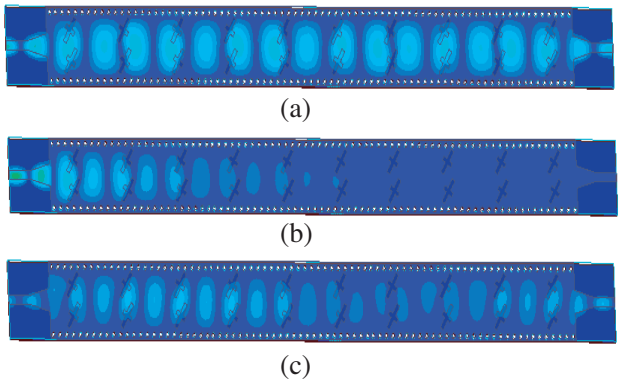

Figure 6. Electric field distribution at different frequencies for the SIW leaky-wave antenna. (a) 10.4 GHz, (b) 13.5 GHz at the transition point, and (c) 15.33 GHz.

Figure 7. Fabricated prototype of asymmetrical LWA.

results (from Anyss HFSS). Good Agreement is observed between them. The parameters are lower than -10 dB in the frequency range of 10 GHz to 15.5 GHz. Due to additional reflections caused by the SMA connectors, the measured S_{11} spectrum differs from simulated ones.

E-field distributions are plotted in Fig. 9 at different frequencies showing the mitigation of the OSB at broadside frequency. The good matching is achieved in the overall frequency range as observed from the E field distributions.

Figure 10 shows the simulated main beam scanning angle of the proposed LWA. The beam scanning angle is achieved from $-40°$ to $+16°$. The simulated beam scanning angle (backward) from $-40°$ to $0°$ is achieved across a frequency band of 10.4 GHz–13.5 GHz and the forward scanning range from $0°$ to $+16°$ which can be achieved across a frequency range from 13.5 GHz to 15.33 GHz.

The simulated and measured normalized radiation patterns at different frequencies are shown in

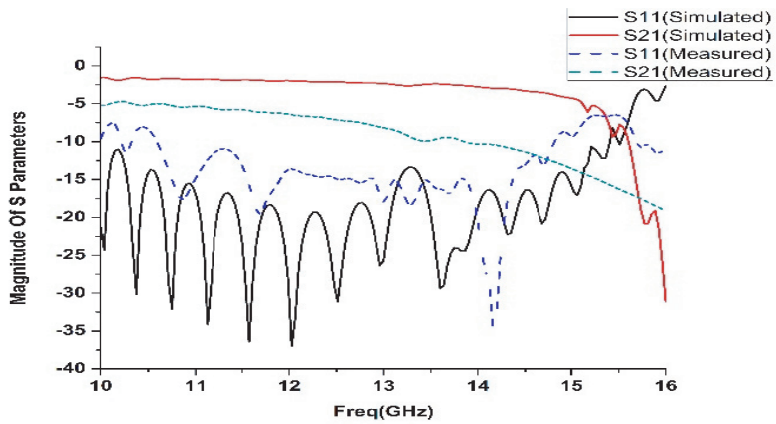

Figure 8. The measured and simulated magnitude of S parameters of the prototype as a function of frequency.

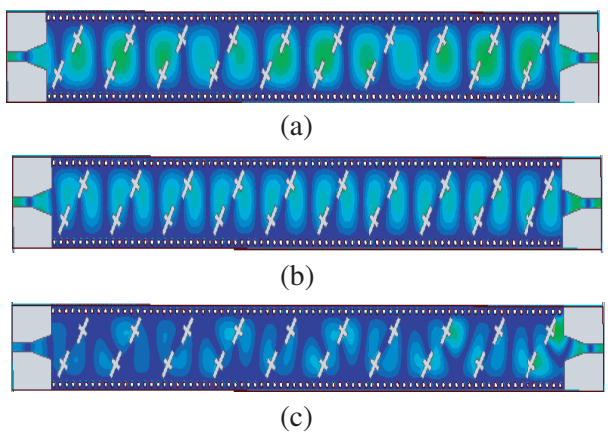

Figure 9. Electric field distribution at different frequencies for the SIW leaky-wave antenna. (a) 10.4 GHz, (b) 13.5 GHz at the transition point, and (c) 15.33 GHz.

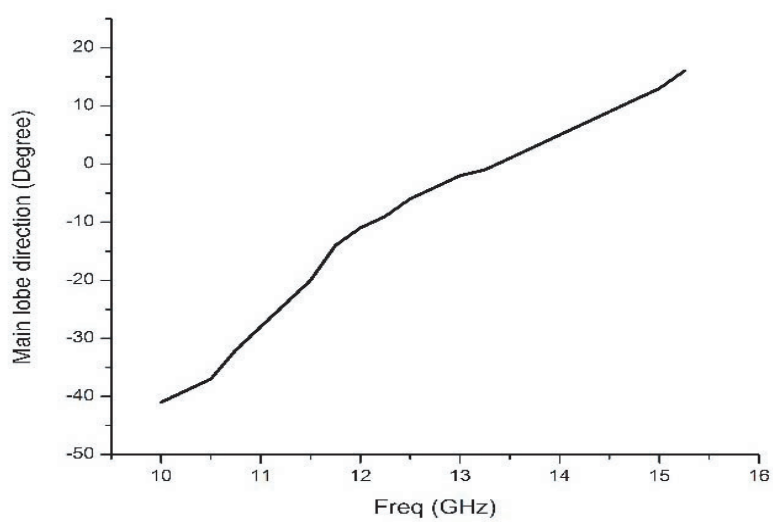

Figure 10. Simulated beam scanning angle with frequency.

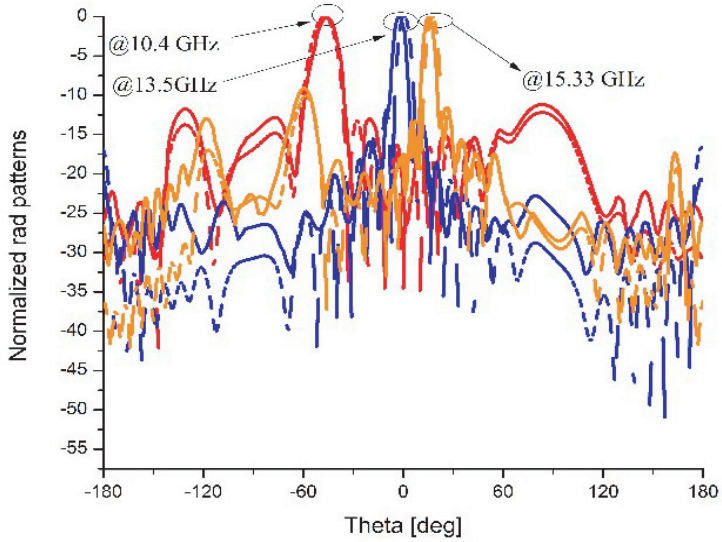

Figure 11. Simulated (dotted) and measured (solid) radiation patterns at different frequency.

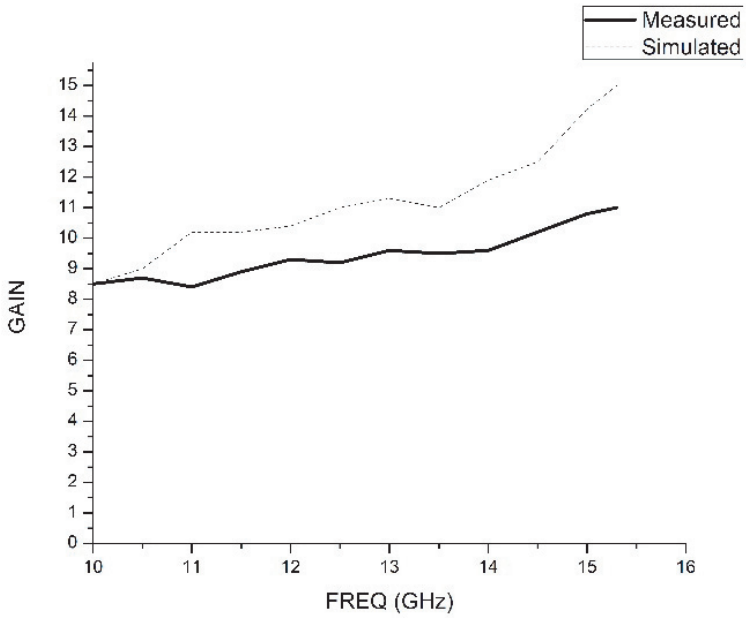

Figure 12. Simulated and measured antenna gains.

Fig. 11. It is seen that the measured results are very close to the simulated patterns for the antenna, although a small discrepancy for the radiation angle due to a shift of frequency is observed. When the frequency is increased, the main beam moves from the backfire towards the end fire direction. At the transition frequency, the radiation goes exactly to the broadside. The results demonstrate that the main radiation beam of the prototype scans at least from $-40°$ at 10.4 GHz to $+16°$ at 15.33 GHz with smooth transition through broadside at 13.5 GHz. The side lobe levels (SLL) are also below -10 dBi. The measured and simulated gains are depicted in Fig. 12. The maximum gain realized for the prototype is 11 dBi. The variation of the gain in the continuous beam scanning form backward to forward range is due to the unequilization of the radiation efficiency.

The features of the proposed SIW LWA are shown in Table 2.

Table 2. Features of the proposed LWA.

S. No	Feature	Proposed SIW LWA
1.	Operating Range	10 GHz–15.5 GHz
2.	Beam Scanning	$-40°$ to $+16°$
3.	Maximum Gain	11 dBi
4.	FSLL	-10 dBi

5. CONCLUSION

A substrate integrated waveguide leaky wave antenna with cross-shaped slots with continuous beam scanning is proposed. By introducing asymmetry in the position of the slots, the mitigation of the OSB is achieved. A 1-D periodic array of the proposed unit cell is fabricated which shows the continuous beam scanning in a wide range of $-40°$ to $+16°$ for the frequency scan of 10 GHz to 15.5 GHz. The maximum realized gain for the prototype is 11 dBi.

ACKNOWLEDGMENT

This work is supported by the Defence Research & Development Organization (DRDO) of India Grant ERIP/ER/1403170/M/01/1555.

REFERENCES

1. Jackson, D. R., C. Caloz, and T. Itoh, "Leaky-wave antennas," *Proc. IEEE*, Vol. 100, No. 7, 2194–2206, 2012.
2. Liu, J., D. R. Jackson, and Y. Long, "Substrate integrated waveguide (SIW) leaky-wave antenna with transverse slots," *IEEE Trans. Antennas Propag.*, Vol. 60, No. 1, 20–29, 2012.
3. Liu, J., X. Tang, Y. Li, and Y. Long, "Substrate integrated waveguide leaky-wave antenna with H-shaped slots," *IEEE Trans. Antennas Propag.*, Vol. 60, No. 8, 3962–3967, 2012.
4. MacHac, J., "SIW leaky wave antennas," *2014 44th European Microwave Conference (EuMC)*, 448–451, Rome, 2014.
5. Deslandes, D. and K. Wu, "Integrated microstrip and rectangular waveguide in planar form," *IEEE Microw. Wirel. Components Lett.*, Vol. 11, No. 2, 68–70, 2001.
6. Design, A. C., E. P. Systems, and T. Systems, *Handbook of Antenna Technologies*, 2014.
7. Xu, F. and K. Wu, "Understanding leaky-wave structures: A special form of guided-wave structure," *IEEE Microw. Mag.*, Vol. 14, No. 5, 87–96, 2013.
8. Caloz, C., "A ten-year journey in leaky-wave antennas," *2015 IEEE Conference on Antenna Measurements & Applications (CAMA)*, 31–34, Thailand, 2015.
9. Otto, S., A. Al-Bassam, A. Rennings, K. Solbach, and C. Caloz, "Transversal asymmetry in periodic leaky-wave antennas for bloch impedance and radiation efficiency equalization through broadside," *IEEE Trans. Antennas Propag.*, Vol. 62, No. 10, 5037–5054, 2014.
10. Lyu, Y.-L., X.-X. Liu, P.-Y. Wang, D. Erni, Q. Wu, C. Wang, N. Y. Kim, and F.-Y. Meng, "Leaky-wave antennas based on non-cutoff substrate integrated waveguide supporting beam scanning from backward to forward," *IEEE Trans. Antennas Propag.*, Vol. 64, No. 6, 2155–2164, 2016.
11. Nasimuddin, Z. N. Chen, and X. M. Qing, "Dual metamaterials substrate integrated leaky-wave structures for antenna applications," *2012 7th Eur. Microw. Integr. Circuits Conf. (EuMIC)*, 830–833, Amsterdam, 2012.
12. Nasimuddin, Z. N. Chen, and X. M. Qing, "Multilayered composite right/left-handed leaky-wave antenna with consistent gain," *IEEE Trans. Antennas Propag.*, Vol. 60, No. 11, 5056–5062, 2012.

13. Nasimuddin, Z. N. Chen, and X. Qing, "Substrate integrated metamaterial-based leaky-wave antenna with improved boresight radiation bandwidth," *IEEE Trans. Antennas Propag.*, Vol. 61, No. 7, 3451–3457, 2013.
14. Nasimuddin, Z. N. Chen, and X. M. Qing, "Tapered composite right/left-handed leaky-wave antenna for wideband broadside radiation," *Microw. Opt. Technol. Lett.*, Vol. 57, No. 3, 624–629, 2015.
15. Nasimuddin, Z. N. Chen, and X. M. Qing, "Slotted SIW leaky-wave antenna with improved backward scanning bandwidth and consistent gain," *2017 11th European Conference on Antennas and Propagation (EUCAP) Conf. Proceedings*, 752–755, France, 2017.
16. Yang, N., C. Caloz, and K. Wu, "Full-space scanning periodic phase-reversal leaky-wave antenna," *IEEE Trans. Microw. Theory Tech.*, Vol. 58, No. 10, 2619–2632, Oct. 2010.
17. Caloz, C., A. Lai, and T. Itoh, "The challenge of homogenization in metamaterials," *New J. Phys.*, Vol. 7, No. 167, 1001–1004, 2005.
18. Pozar, D. M., *Microwave Engineering*, 4th Edition, Wiley, 2011.
19. Collin, R. E., *Foundations for Microwave Engineering*, Wiley-IEEE Press, Dec. 2000.
20. Xu, F. and K. Wu, "Guided-wave and leakage characteristics of substrate integrated waveguide," *IEEE Trans. Microwave Theory Tech.*, Vol. 53, No. 1, 66–73, 2005.
21. Rayas-Sánchez, J. E., "An improved em-based design procedure for single-layer substrate integrated waveguide interconnects with microstrip transitions," *2009 IEEE MTT-S Int. Microw. Work. Ser. Signal Integr. High-Speed Interconnects, IMWS*, 27–30, Mexico, 2009.
22. Gomez-Diaz, J. S., A. Alvarez-Melcon, and J. Perruisseau-Carrier, "Analysis of the radiation characteristics of CRLH LWAs around broadside," *2012 6th Eur. Conf. on Antennas and Propagation (EUCAP)*, 2876–2880, Prague, 2012.
23. Caloz, C. and S. Otto, "A tour on recent developments and discoveries of crucial practical importance in leaky-wave antennas," *2013 European Microwave Conference (EuMC)*, 495–498, Germany, 2013.
24. Suntives, A. and S. V. Hum, "An electronically tunable half-mode substrate integrated waveguide leaky-wave antenna," *2011 5th Eur. Conf. Antennas and Propagation (EuCAP)*, 3670–3674, Rome, 2011.